Journal of the European Ceramic Society 15 (1995) 1125–1134

0955-2219(95)00083-6
0955-2219/95/$9.50

Moisture Sensitive Degradation in TiO_2–Y_2O_3–ZrO_2

A. E. Hughes,[a]* H. St John,[b] P. Kountouros[c]† & H. Schubert[c]

[a]C.S.I.R.O., Division of Materials Science and Technology, Private Bag 33, Rosebank MDC, Clayton, 3169, Victoria, Australia
[b]C.S.I.R.O., Division of Chemicals and Polymers, Private Bag 33, Rosebank MDC, Clayton, 3169, Victoria, Australia
[c]Max-Plank-Institut für Metallforschung, Institut für Werkstoffwissenschaft, Pulvermetallurgisches Laboratorium, Heisenbergstraße 5, 7000 Stuttgart 80, Germany

(Received 19 January 1995; revised version received 18 May 1995; accepted 19 May 1995)

Abstract

Sintered discs (1450°C) of yttria–stabilised tetragonal zirconia (3 mol% Y_2O_3) with additions of 1, 10 and 20 mol% TiO_2, were treated in distilled water in an autoclave at 170°C for times up to 144 h. X-ray diffraction (XRD) and X-ray photoelectron spectroscopy (XPS) were used to monitor changes which occurred at the surface of the discs during autoclave treatment. The addition of TiO_2 retarded the transformation of the tetragonal (t)-phase to monoclinic (m)-phase as determined by XRD. During autoclave treatment an increase in the Ti/Zr ratio, decrease in the Y/Zr ratio and a peak in the percentage Zr^{3+} were observed using XPS. Furthermore, at long autoclave treatment times there was a surface oxygen enrichment in excess of that expected from the stoichiometry. The data have been interpreted in terms of vacancy annealing and the rate of transformation to m-ZrO_2 appears to be related to the presence of Zr^{3+}, adsorbed water and substitutional cations such as Ti^{4+} in modifying adsorption sites at the surface.

1 Introduction

Sintered and fully dense Y_2O_3–stabilized tetragonal zirconia polycrystal (Y–TZP) undergoes an unusual surface degradation at low temperatures (100–500°C) during exposure to air saturated with water vapour or autoclave treatment. The degradation is most pronounced at ~250°C and is characterized by a loss of mechanical properties[1–4] as a result of microcracking, spalling or even complete collapse of the sintered body.[5–8] The surface degradation has been shown to be due to transformation of the surface tetragonal (t) grains to monoclinic (m) phase and the microcracking results from the volume expansion associated with the transformation to the m-phase. Hence the longer the exposure time to moist environments the deeper the transformation zone and the more dire the consequences for the mechanical properties of the sintered bodies.[2,6–11]

The amount of transformation depends on grain size and yttria content of the Y–TZP.[5,11] For example, Watanabe *et al.*[3] found that the critical grain size below which no transformation occurred, increased from 0·2 to 0·6 μm as the yttria content of the Y–TZP increased from 2 to 5 mol% Y_2O_3. As the yttria content is increased the t-phase becomes more stable on a thermodynamic basis and consequently there is less transformation to the m-phase.[2,5]

Various models have been proposed to explain the low-temperature degradation of Y–TZP. Lange *et al.*[11] suggested that α-$Y(OH)_3$ formation created yttria-poor regions at grain surfaces which act as nucleation sites for the m-phase. Sato and Shimada[12] proposed that water vapour attack at pre-existing flaws resulted in crack propagation by scission of Zr–O–Zr bonds and formation of Zr–OH, releasing the strain which stabilizes the t-phase thus promoting the t→m transformation. Similarly, Yoshimura[13,14] proposed that water attack produces scission of the bridging surface oxygen groups resulting in Zr–OH or Y–OH formation thus opening up the subsurface region to further attack by H_2O and eventual crack propagation. However, in his case it was a stress corrosion cracking mechanism since the stress field at the crack tip induces the t→m transformation.

Another class of models considers the destabilization of the t-phase via annealing of the anion vacancies with a range of species, i.e. occupation

*Author to whom correspondence should be addressed.
†Present Address: Research Centre Jülich, Institute for Materials in Energy Systems, D-52425, Jülich, Germany.

of the anion vacancies with anions. Narita *et al.*[15] suggested that water reacts with anion vacancies to produce interstitial hydrogen ions and oxygen anions which occupy anion vacancies (annealing) leading to the destabilization of the t-phase. Hughes *et al.*[8] also concluded that the moisture sensitivity of Y–TZP was related to annealing of anion vacancies by O^{2-} anions. In their experiments they observed an increase in the oxygen anion/zirconium ratio during exposure to moist air at 200°C using X-ray photoelectron spectroscopy (XPS). Lepitso and Māntylā[10] also concluded that anion vacancy annealing by O^{2-}accompanied by grain boundary attack, promoted the t→m transformation. Kountouros and Petzow[16] have shown that oxygen vacancies play a decisive role in the stability of the t-phase (and c-phase) and argue that vacancy annealing by oxygen anions promotes the t→m transformation. Furthermore elastic recoil detection analysis (ERDA) spectra on TZP-samples degraded in D_2O-rich water have shown that H- and D-atoms penetrate the lattice.[17]

Much effort has been devoted to reducing or even eliminating the low-temperature degradation effect. In a number of studies the effects of different substitutional cations have been examined. For example, Sato and Shimada[18] observed that Al_2O_3 or CeO_2 additions provided some degree of control of the moisture sensitive degradation. Based on free energy considerations they concluded that the t-phase was stabilized, in the case of Al_2O_3 addition, by increasing the strain energy of the constraining matrix and for alloying with CeO_2 by increasing the chemical free energy. XPS studies by Theunissen *et al.*[19] and Duran *et al.*[20] suggested that protection of the t-phase in ternary systems containing CeO_2 and TiO_2 was imparted by surface segregation of Ce^{4+} and Ti^{4+} and formation of protective overlayers on the external surface and possibly in the grain boundary. Kountouros and Petzow[16] have noted that the activation energy for total ionic conductivity increases significantly in the presence of Ti^{4+} hence oxygen anions may become 'locked' in lattice sites due to changed bonding conditions. Under such circumstances, if there is surface enrichment of Ti^{4+} a semi-impenetrable 'vacancy-annealed barrier' may be set up protecting the interior of the grain from further vacancy annealing and consequently retarding the transformation to the m-phase.

The development of such a large variety of models to describe the one phenomenon is a consequence of the limited control over processing variables during sample preparation which significantly alter the microstructure and consequently the extent of transformation. Processing variables such as sintering times, temperatures and atmospheres can significantly alter; grain growth, average grain size, grain size distributions, yttria disproportionation, impurity phase distribution within the grain boundary network and soluble impurity distributions within grains. Furthermore, many spectroscopic studies have examined the surfaces of degraded specimens only after severe treatments rather than during transformation. For example, it is only *after* extensive autoclave or moist air treatment that either hydroxide formation has been observed using XPS[7,10,20] or significant OH^- formation has been observed using Fourier Transform Infrared (FTIR) spectroscopy.[13,15,21]

In this paper the authors have examined the effects of the addition of Ti^{4+} as a substitutional cation for Z^{4+}, on the stability of Y–TZP during autoclave treatment at 170°C. X-ray diffraction (XRD) has been used to monitor the generation of the m-phase, while XPS has been used to study chemical changes at the surface.

2 Experimental

2.1 Sample preparation

The details of preparation of the TiO_2–Y_2O_3–ZrO_2 samples has been given in detail elsewhere.[22] Briefly, powders were prepared by co-precipitation during spraying of chloride solutions of $ZrOCl_2.8H_2O$, $YCl_3.6H_2O$ and $TiCl_3$ mixed in the required stoichiometry into ammonia solution. The precipitate was then washed several times in distilled water to ensure that it was Cl^- free, distilled azeotropically to dehydrate the powder and dried at 70°C. The powder was calcined at 950°C for 3 h, wet milled in ethanol with TZP balls, dried at 70°C and pressed into 1 × 1 cm cylinders at either 200 or 630 MPa. These cylinders were sintered in air by ramping at 100–1450°C, cooled, then cut, lapped and polished to a 1 μm finish. The three compositions of interest here had 3 mol% Y_2O_3 and either 1, 10 or 20 mol% TiO_2 and are designated Z3Y1T, Z3Y10T and Z3Y20T respectively. The samples were prepared in Germany and transported to Australia for analysis.

2.2 Autoclave treatments

The discs were subsequently placed in 40 cc of distilled water in an autoclave for times up to 144 h, which represented surface saturation of m-ZrO_2, at 170°C (0·792 MPa). After each treatment time the specimens were removed, examined by XRD and XPS, then given further autoclave treatment in fresh distilled water.

2.3 X-ray diffraction (XRD)

The m-phase content was determined by XRD using the (111)m, (11$\bar{1}$)m and (111)t reflections (Cu Kα radiation). In a preliminary series of experiments the development of m-ZrO_2 in the polished surface of Z3Y10T was monitored using XRD without any XPS experiments being made on the specimens. In subsequent series of experiments both XRD and XPS measurements were made on specimens of all compositions at each autoclave treatment time. No difference was found in the amount of m-phase generated with either the XRD or the XRD followed by XPS series of experiments, therefore the XPS has no effect on the generation of m-phase.

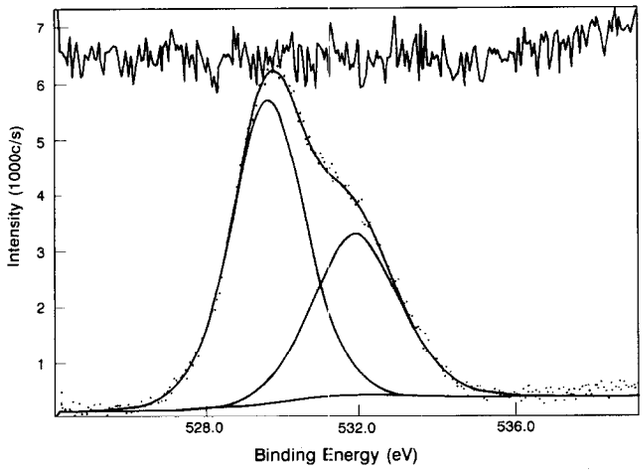

Fig. 1. Typical fit of Gauss/Lorentz product functions to an O 1*s* spectrum. Spectrum of Z3Y10T after 7 h treatment in an autoclave at 170°C. Oxygen anions contribute to the low binding energy component while adsorbed water or O_2^- contribute to the high binding energy component. Reduced χ^2 = 1·012 with 170 degrees of freedom.

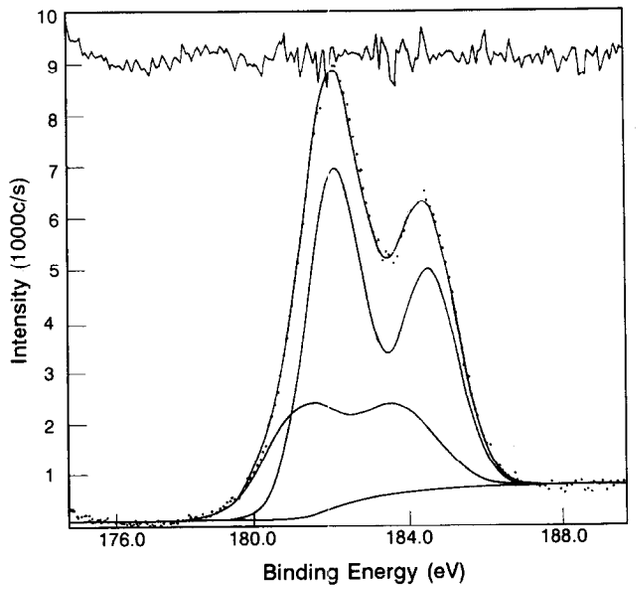

Fig. 2. Typical fit of doublets comprised of two Gauss/Lorentz product functions to a Zr 3*d* spectrum. Spectrum of Z3Y10T after 0·5 h treatment in an autoclave at 170°C. Zr^{3+} moieties contribute to the low binding energy component while Zr^{4+} cations contribute to the high binding energy component. Reduced χ^2 = 1·099 with 140 degrees of freedom.

2.4 X-ray photoelectron spectroscopy (XPS)

The experimental setup and quantification of results for XPS has been described previously.[23] Extensive analysis was made of the O 1*s* and Zr 3*d* spectra by curvefitting Gauss/Lorentz product functions. Two components, without any constraints, were fitted to each O 1*s* spectrum (Fig. 1). Two unconstrained Zr 3*d* doublets were fitted to the Zr 3*d* spectra. The Z_r^{4+} doublet had a fixed separation of 2·42 eV and relative intensity of 0·686, whereas the Zr^{3+} doublet had the same separation but the relative intensity was allowed to float and typically reached values of 0·8. The origin of this small additional intensity is not clear. A typical fit to the Zr 3*d* region is shown in Fig. 2.

3 Results

The %m-ZrO_2 generated in Z3Y1T, Z3Y10T and Z3Y20T as a function of treatment time in the autoclave at 170°C is presented in Fig. 3. It is clear that the development of the m-phase is retarded by increasing the TiO_2 content of the Y_2O_3–ZrO_2. Z3Y1T reached a saturation value of around 78%m-ZrO_2 after only 20 h treatment whereas the times to saturation with m-ZrO_2 for Z3Y10T and Z3Y20T was increased to around 70 and 144 h respectively.

It is important to note that because of the surface sensitivity of XPS, changes in the atomic ratios only reflect changes that occur in the surface grains. Hence it is worth attempting to estimate at what stage all surface grains have transformed to the m-phase. Assuming the analysis depth of XRD is approximately 7 μm[24] and the grain size and saturation value of m-phase are 1·3 μm and 78% respectively then the surface should be fully transformed between 7 and 8% m-ZrO_2, assuming transformation to a depth corresponding to half average grain size. (Recall that the surface is

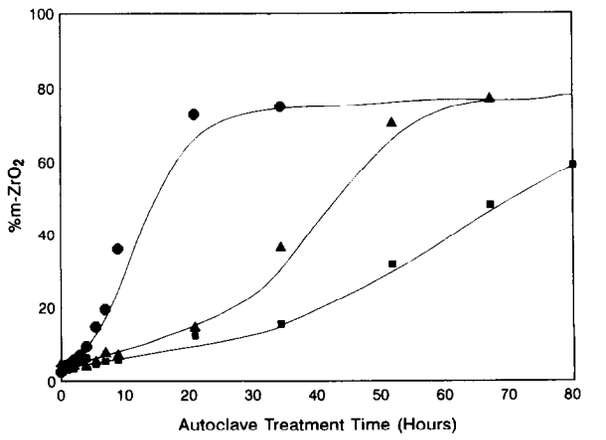

Fig. 3. %m-ZrO_2 phase content of the surface determined by XRD versus the autoclave treatment time at 170°C. (●) Z3Y1T; (▲) Z3Y10T and (■) Z3Y20T.

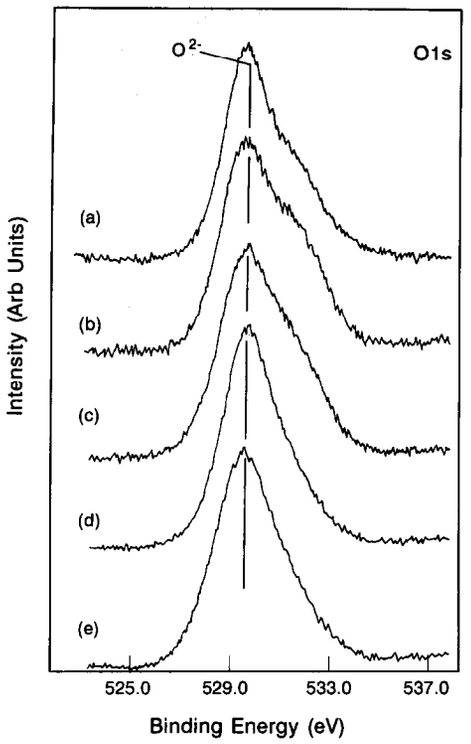

Fig. 4. Series of O 1*s* spectra displaying changes which occur as a result of autoclave treatment. (a) 0; (b) 4; (c) 7; (d) 9 and (e) 34 h.

polished so the surface layer is only half the average grain size in thickness.)

XPS measurements were made on the discs of Z3Y1T, Z3Y10T and Z3Y20T after each treatment time in the autoclave. It can be seen in Fig. 4 that significant changes occurred to the O 1*s* spectra as a function of autoclave treatment time as indicated by a change in the relative intensity from low to high binding energies. Curvefitting of the O 1*s* spectra revealed the presence of two components at 529·8 eV (O_I) and 532·2 eV (O_{II}). Previously four component fits were made to 3 mol%Y_2O_3–ZrO_2 after treatment in moist air at 200°C,[8,24] however, in this case no statistically significant fits could be obtained with either three or four components. The component O_I at 529·8 eV is typical of oxygen anions in lattice sites.[23,25] Adsorbed water[26] or O_2^-[27] are likely candidates for the O_{II} component at 532·2 eV. Hernandez *et al.*[7,20] attributed a high binding energy component at 532·8 eV in autoclave treated CeO_2–Y_2O_3–ZrO_2 to bound hydroxyl groups based on hydroxylation of transition metal compounds. However surface hydroxides on zirconia or yttria occur around 531 eV[28] and are unlikely to contribute to the O_{II} intensity. Likewise O_2^{2-}, which may be present on the surface, occurs at around 531·2 eV and therefore is unlikely to contribute to O_{II}.[28]

The dependence of the total oxygen to zirconium (O_{TOT}/Zr) atomic ratio as well as O_I/Zr and O_{II}/Zr on the autoclave treatment time are plotted

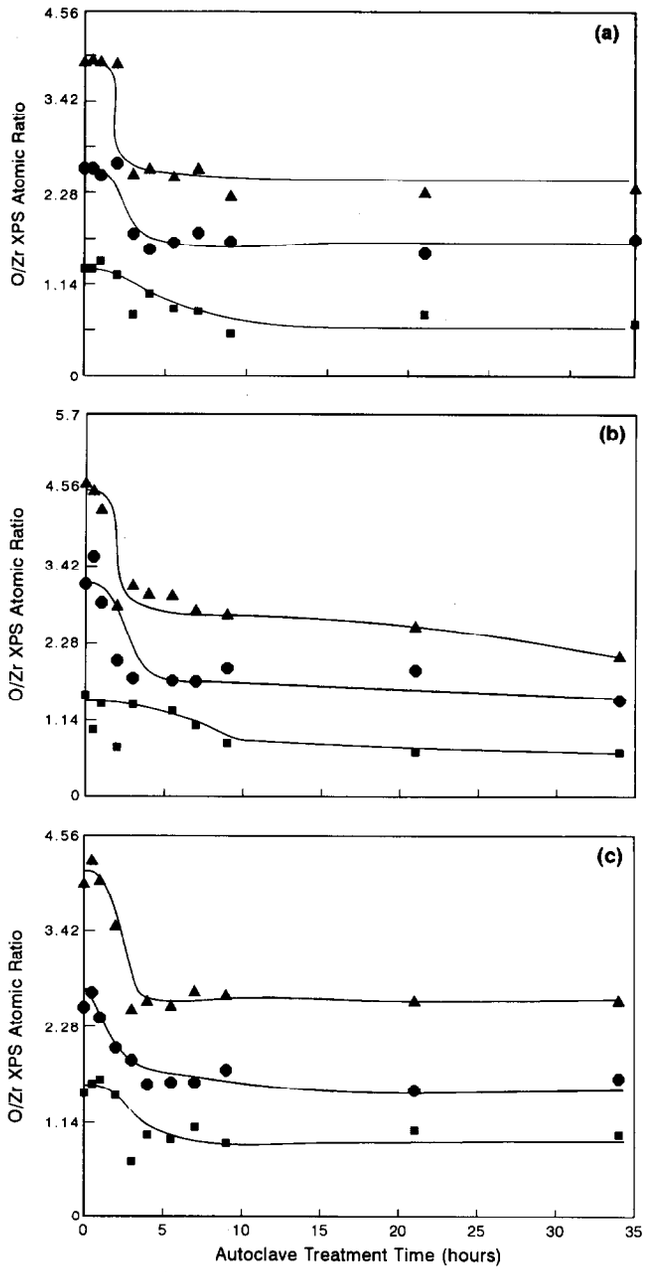

Fig. 5. (▲) O_{TOT}/Zr; (●) O_I/Zr low binding energy component due to oxygen anions and (■) O_{II}/Zr high binding energy component due to adsorbed water as a function of autoclave treatment time. (a) Z3Y1T; (b) Z3Y10T and (c) Z3Y20T.

in Figs 5(a)–(c). The O/Zr ratios displayed stepwise decreases between 1 and 2 h treatment time for Z3Y1T (Fig. 5(a)) and 2 and 3 h for Z3Y10T (Fig. 5(b)) and Z3Y20T (Fig. 5(c)) respectively. The stepwise decrease was partially obscured when the data were plotted as a function of %m-ZrO_2 suggesting that the loss of oxygen is not caused by the development of the m-phase. Indeed, the decreases occurred at much shorter times than those expected for surface saturation of the m-phase and most likely resulted from the removal of some surface carbon contamination of the specimens which may have originated during polishing and/or storage and transport. In the

presence of a carbon overlayer the high O/Zr ratios are most likely explained on the basis that the XPS is sampling a much smaller volume of the actual ceramic surface than for a material without the contaminating layer. (This was confirmed in repeat experiments on freshly polished surfaces where very little carbon was detected on the surface and the O/Zr ratio was around 1·8.) This would enhance the O/Zr signal since the external surface of the ceramic is oxygen rich. The O_{II} component displayed only a gradual decrease with increasing treatment time indicating an apparent reduction in the amount of adsorbed water. However, the $\%O_{II}$ of O_{TOT} goes through a peak as a function of autoclave treatment (Fig. 6).

Increasing autoclave treatment time also resulted in a loss of resolution in the normally well resolved Zr 3*d*5/2–3*d*3/2 spin-orbit doublet of the Zr 3*d* spectra, suggesting the presence of additional components (Fig. 7). These changes can be demonstrated, for example, by comparing the apparent loss of resolution of the Zr 3*d*5/2 and 3/2 doublet in Z3Y10T before autoclave treatment (Fig. 7(a)) with 4 and 7 h autoclave treatment at 170°C (Figs 7(b) and (c) respectively). Curve fitting of the Zr 3*d* spectra revealed two components corresponding to Zr^{4+} (182·2 ± 0·1 eV) and a second component at 181·4 ± 0·2 eV most probably due to the presence of Zr^{3+} (Fig. 2).[29,30]

Hughes *et al.*[24] have previously argued that the origin of the Zr^{3+} signal is most likely related to trapping of electrons at associated cation-vacancy pairs. Electron spin resonance (ESR) measurements indicate that associated vacancy-Zr cation moieties are efficient traps for low energy electrons.[31,32] The electron becomes trapped in the *d*-orbital resulting in a $4d^1$ configuration and Zr^{3+}. One source of low-energy electrons is the XPS experiment itself where photoelectrons undergo inelastic interactions within the solid thereby losing much of their kinetic energy. A second source of low energy electrons may arise with the exchange of O^{2-} with O_2. The broad 1/2 width of the low

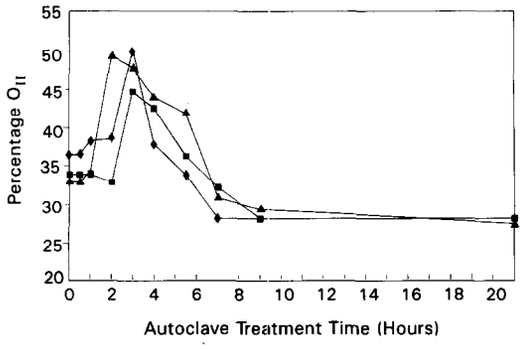

Fig. 6. Variation of $\%O_{II}$ with autoclave treatment time. (■) Z3Y1T, (▲) Z3Y10T and (♦) Z3Y20T.

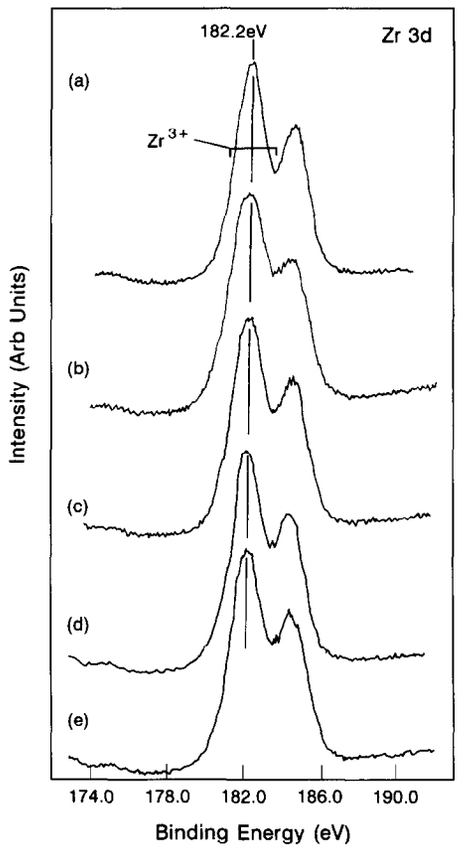

Fig. 7. Series of Zr 3*d* spectra displaying changes which occur as a result of autoclave treatment. (a) 0; (b) 4; (c) 7; (d) 9 and (e) 34 h.

binding energy Zr 3*d* component reflects a variety of Zr^{3+} configurations (Fig. 2). Regardless of their origin, these Zr^{3+} sites are important from the viewpoint of surface chemistry since ESR measurements indicate that they are co-ordinatively unsaturated but can co-ordinatively saturate through adsorption of species such as H_2O.[33,34]

The % Zr^{3+} determined from curvefitting, as a function of treatment time at 170°C is presented in Fig. 8. (As with the O/Zr ratios the $\%Zr^{3+}$ displayed no correlation with $\%m\text{-}ZrO_2$ phase content.) Although there is some scatter in the data it would seem that at short autoclave treatment

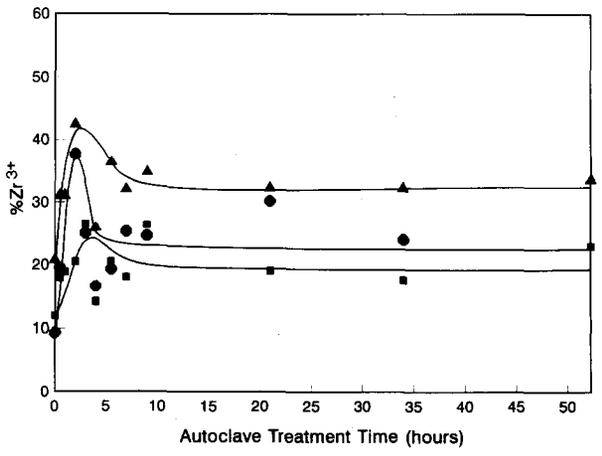

Fig. 8. % Zr^{3+} as a function of the autoclave treatment time at 170°C. (▲) Z3Y1T, (●) Z3Y10T and (■) Z3Y20T.

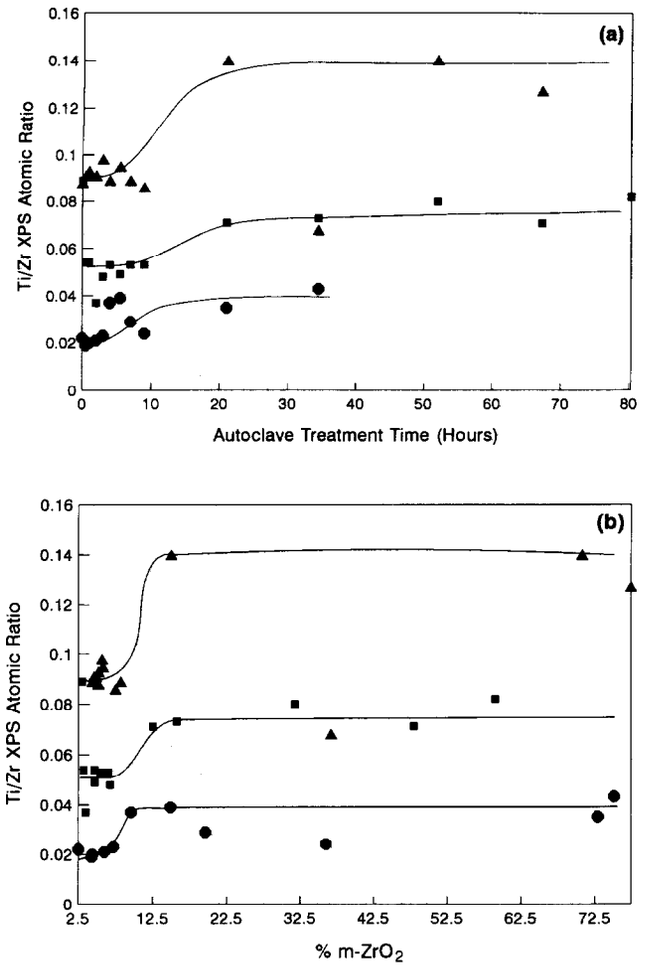

Fig. 9. Ti/Zr ratio versus (a) autoclave treatment time and (b) %m-ZrO_2. (●) Z3Y1T (■) Z3Y10T and (Δ) Z3Y20T.

times (between 2 and 4 h) there is a peak in the $\%Zr^{3+}$ but thereafter it remains constant. The peak maxima appear to be highest for Z3Y1T and Z3Y10T at around 40% Zr^{3+} but considerably less for Z3Y20T at approximately 25% Zr^{3+}.

While the O/Zr ratios and $\%Zr^{3+}$ appeared to depend primarily on the autoclave treatment time, the Ti/Zr ratios were a function of the m-phase content of the surface as clearly demonstrated in Fig. 9. The Ti/Zr ratios remained constant over the first few hours of autoclave treatment then exhibited a stepwise increase to new equilibrium values but this step was staggered in the time domain for the different compositions (Fig. 9(a)), but occurred in the single range 7–13%m-ZrO_2 for all compositions (Fig. 9(b)) which spans the region where there is complete saturation of the surface with m-phase.

The initial and final Ti/Zr atomic ratios are presented in Table 1 and compared to those expected from the stoichiometries of the different ceramics. For Z3Y1T all measured values of the Ti/Zr ratio indicate a surface enrichment of Ti^{4+}. The Ti/Zr ratio for untreated Z3Y10T indicated a small surface depletion of Ti^{4+}, which changed to enrichment after autoclave treatment. Severe surface depletion of Ti^{4+} was observed under all conditions for Z3Y20T. Z3Y10T exhibited nearly twice the level of surface Ti^{4+} compared to Z3Y20T which itself was twice the level of the Z3Y1T specimen, suggesting that there is a TiO_2 content which will give a maximum surface Ti enrichment. This is demonstrated in Fig. 10 where the Ti/Zr ratio displayed a clear maximum at 5 mol% TiO_2 for the as-sintered specimens.

Table 1. XPS and calculated Ti/Zr ratios after various treatments

Sample	*Untreated*[1]	*Treated*[2]	*Expected*[3]
Z3Y1T	0·022	0·038	0·010
Z3Y10T	0·088	0·14	0·115
Z3Y20T	0·055	0·079	0·26

[1]XPS atomic ratio measured on the surface prior to autoclave treatment.
[2]XPS atomic ratio measured after autoclave treatment for longer than 30 h.
[3]Calculated on the basis of bulk stoichiometry.

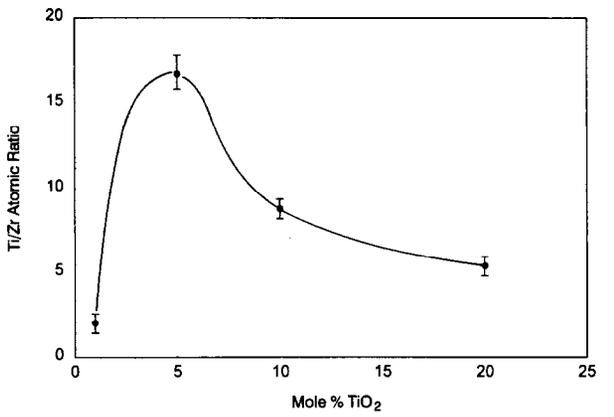

Fig. 10. Surface Ti/Zr ratio (by XPS) versus the bulk mol% TiO_2.

The Y/Zr ratios also displayed significant changes around 7% m-ZrO_2 phase content of the surface (Fig. 11). The initial and final values of the Y/Zr ratios are compared to the expected values in Table 2. The Y/Zr ratios for the untreated samples

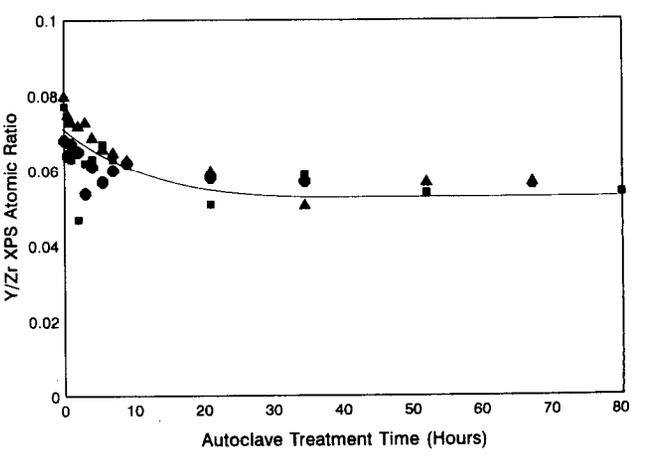

Fig. 11. Y/Zr ratio versus autoclave treatment time. (●) Z3Y1T, (▲) Z3Y10T and (■) Z3Y20T.

Table 2. XPS and calculated Y/Zr ratios after various treatments

Sample	*Untreated*[1]	*Treated*[2]	*Expected*[3]
Z3Y1T	0·068	0·058	0·0625
Z3Y10T	0·080	0·057	0·0690
Z3Y20T	0·077	0·055	0·0780

[1]XPS atomic ratio measured on the surface prior to autoclave treatment.
[2]XPS atomic ratio measured after autoclave treatment for longer than 30 h.
[3]Calculated on the basis of bulk stoichiometry.

all displayed either surface enrichment or ratios similar to the expected bulk values. After autoclave treatment all compositions displayed a depletion to a common value of around 0·057 ± 0·004.

4 Discussion

The most notable features of the XPS data were the decrease in the Y/Zr ratio and peaks in the $\%Zr^{3+}$ during the first 3 h treatment for all samples. Furthermore, there was an increase in the Ti/Zr ratio between 7 and 13%m-ZrO_2, a range which represents the complete transformation of surface grains to m-phase. These changes suggest that some local surface rearrangements must occur with respect to the starting compositions of the material. It would appear that these changes occur during a period where the surface is undergoing transformation to the m-phase but thereafter no further changes are observed.

The XPS data clearly deals with two different phenomena:

(i) Changes in the O/Zr ratios, particularly the $\%O_{II}$, and the % Zr^{3+}, which only depend on the autoclave treatment time and thus may herald changes in the surface chemistry which lead to the t→m phase transformation;
(ii) Changes in the Ti/Zr and possibly the Y/Zr ratios which are associated with cation redistribution as part of the m-phase transformation.

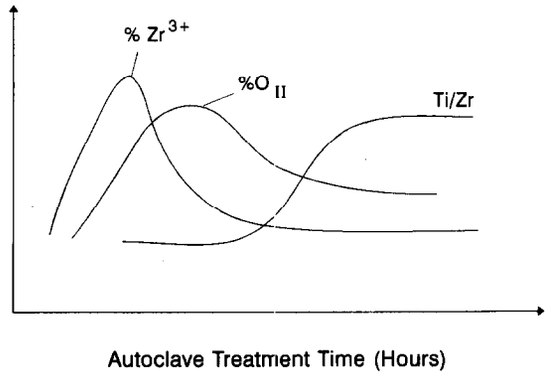

Fig. 12. Schematic representation of the temporal evolution of changes in the surface chemistry.

These changes are summarised schematically in Fig. 12.

4.1 Generation of Zr^{3+} and O_2^-

Changes in the surface chemistry appear to begin with an increase in the level of Zr^{3+} which is followed by an apparent change in the degree of occupation of surface anion sites by the O_{II} species (adsorbed water and probably superoxide). At much longer autoclave treatment times, where the surface is fully saturated with m-ZrO_2, the Ti/Zr ratios increase suggesting cation redistribution as a result of phase transformation.

In order to understand these changes this discussion will begin with the role of the Zr^{3+} sites and their influence on the O_{II} species drawing on the ESR studies of adsorbed H_2O and O_2^- on m-ZrO_2. Morterra *et al.*[33,34] have identified a number of different surface species and adsorption sites on m-ZrO_2. One of the important adsorption sites being the co-ordinatively unsaturated (cus)-Zr^{3+} centres which can co-ordinatively saturate in the presence of water without oxidizing to Zr^{4+}. Furthermore, the Zr^{3+} centres were not quenched by the presence of superoxide from which they concluded that the electron donating centres which gave rise to O_2^- at the surface, must be ESR silent. (They suggested that O_2^- was formed by donation of electrons from the conduction band.) This indicates that the Zr^{3+} centres which co-ordinatively saturate with H_2O and sites where O_2^- occur must coexist. In addition, they found that superoxide (O_2^-) formation on m-ZrO_2 is an activated process which only occurred in appreciable amounts at 150°C. In the presence of water, the activation barrier for superoxide formation was reduced and considerable quantities of superoxide were formed at room temperature.

In the work of Morterra *et al.*[33] the Zr^{3+} centres were generated by annealing in vacuum or O_2 at temperatures between 375 and 825°C. In the autoclave, the Zr^{3+} centres are most likely produced in the normal process of exchange of O^{2-} with atmospheric O_2 except that, in the autoclave environment, water molecules are also present and compete for surface sites. Consequently, it is likely that a considerable proportion of the surface Zr^{3+} sites become coordinatively saturated with water. In the presence of an increased density of adsorbed water on the surface of the ceramic much more O_2^- will be generated. Since the generation of O_2^- is the first step in the reduction of oxygen it is assumed that the presence of superoxide will lead ultimately, to much more O^{2-} than would occur on a surface largely free of adsorbed water. Some indirect evidence for the relationship between adsorbed water and the cus-Zr^{3+} sites is provided

Table 3. O_{TOT}/Zr, $\%O_I/Zr$, $\%O_{II}/Zr$ and $\%Zr^{3+}$ for Z3Y20T after 80 h autoclave treatment at 170°C versus examination time under X-ray source

Time (min)[1]	O_{TOT}/Zr	$\%O_I/Zr$	$\%O_{II}/Zr$	$\%Zr^{3+}$
0–10	2·34	61·5	38·5	26·6
30–40	2·29	65·7	34·3	24·0
60–70	2·29	70·6	29·4	21·8
90–100	2·21	71·5	28·5	19·8

[1]It takes approximately 5 min to measure each of the Zr 3*d* and O 1*s* spectra hence a 10 min window is given for each entry in the table.

by the data in Table 3. During dehydration under the X-ray source, O_{II}/Zr (adsorbed water and superoxide) decreased with a consequent loss of Zr^{3+}. In addition there was evidence to suggest that the O_{II} species may have been converted to O^{2-} since there is a 26% reduction in O_{II} but only a total reduction in O_{TOT} of 5·5%. Furthermore, there is also a 26% reduction in the $\%Zr^{3+}$ indicating that the Zr^{3+} have been oxidized up to Zr^{4+} concurrently with the decomposition of the O_{II} species to oxygen anions. As a result of O^{2-} generation there is rapid annealing of surface vacancies and likely penetration of O^{2-} into the lattice, destabilizing the t-phase and resulting in either transformation to the m-phase or the nucleation of domains of m-phase. The likelihood of m-phase nucleation domains is further improved by surface depletion of Y (Fig. 10).

4.2 Anion annealing

Evidence for anion annealing comes from the data collected at longest autoclave treatment times where all compositions have reached surface saturation with m-phase. The saturation values of O_{TOT}/Zr, O_I/Zr and O_{II}/Zr at these long treatment times are presented in Table 4 along with expected values based on the stoichiometry. Two points need to be made with respect to the table. First, the measured O_{TOT}/Zr ratios are much larger than the ratios calculated on the basis that all the anion vacancies are filled (O/Zr), suggesting the presence of oxygen rich species such as some form of molecular oxygen, perhaps superoxide (O_2^-). Furthermore, O_{TOT}/Zr is higher than the stoichiometries that take into account vacancies due to the presence of either Y^{3+} (O^{Y}_{Vac}/Zr) or Y^{3+} and Zr^{3+} ($O^{Y,Zr3+}_{Vac}/Zr$) suggesting that many of the oxygen vacancies have been filled. Second, O_I/Zr, which only accounts for the oxygen anions in the lattice, falls far short of any of the calculated stoichiometries. It is only with the contribution of O_{II}/Zr that the experimental values approach the values calculated from the stoichiometry suggesting that a significant proportion of the surface oxygen anion sites are occupied by the O_{II} species, i.e. adsorbed H_2O or O_2^-. It is difficult to distinguish adsorbed H_2O from O_2^- using XPS core levels, however, preliminary static secondary ion mass spectrometry (SIMS) spectra confirm the presence of O_2^- after autoclave treatment whereas no O_2^- was evident before treatment on freshly polished surfaces. The SIMS results indicate that superoxide must therefore partially contribute to the O_{II} species observed in XPS.

Table 4. Comparison of XPS O/Zr ratios after long treatment time with the calculated O/Zr ratios

Treatment	*Z3Y1T*	*Z3Y10T*	*Z3Y20T*
O_{TOT}/Zr*	2·36	2·65	2·65
O_I/Zr*	1·66	1·80	1·66
O_{II}/Zr*	0·684	0·857	0·964
O/Zr¶	2·14	2·37	2·68
O^{Y}_{Vac}/Zr§	2·12	2·33	2·63
$O^{Y,Zr3+}_{Vac}/Zr$†	1·82	2·03	2·33

*Average XPS atomic ratio determined after surface saturation with m-phase.

¶Calculated with known molar concentration of oxides assuming that each oxide has its full oxygen stoichiometry, e.g. for Z3Y10T there is 87 mol% ZrO_2, 6 mol% $YO_{1.5}$ and 10 mol% TiO_2 hence the O/Zr ratio is $(2 \times 87 + 2 \times 6 + 2 \times 10)/87 = 2{\cdot}37$.

§Calculated with known molar concentration of oxides assuming that each oxide has its fill oxygen stoichiometry, e.g. for Z3Y10T there is 87 mol% ZrO_2, 6 mol% $YO_{1.5}$ and 10 mol% TiO_2 hence the O/Zr ratio is $(2 \times 87 + 1{\cdot}5 \times 6 + 2 \times 10)/87 = 2.33$.

†Calculated on the basis of bulk stoichiometry but taking into account vacancies created by the presence of Y^{3+} and Zr^{3+}, e.g. for Z3Y10T $(2 \times 87 - 0{\cdot}2 \times 87 + 2 \times 10)/87 = 2{\cdot}03$ where the second term takes account of 20% Zr^{3+} in the Zr 3*d* spectra and assumes that one vacancy is associated with each Zr^{3+}.

4.3 Substitutional cations

The role of substitutional cations emerges; replacement of surface or bulk Zr^{4+} cations by Ti^{4+} or other cations will modify adsorption conditions on the surface. For example, on the rutile form of TiO_2, water adsorption has been reported up to 300°C[35] whereas on anatase water desorbs around 200°C and is dependent on the surface crystallography.[36] On m-ZrO_2 molecular water desorbs from the surface below 200°C.[37] Hence it is possible that stronger binding of chemisorbed water in the presence of Ti^{4+} may suppress the rate of formation of O^{2-}. Furthermore, it has been noted by Kountouros and Petzow[16] that the activation energy for ionic conductivity increases when TiO_2 is used as an alloying component. This suggests that oxygen may be more tightly bound in the modified neighbourhood of Ti^{4+}. Clearly, however, the surface Ti/Zr ratio has little direct bearing on the rate of transformation to the monoclinic phase since Z3Y10T had the highest surface concentration of Ti but transformed at autoclave times intermediate between those of Z3Y1T and Z3Y20T.

It should be noted that while this model is based on the XPS results of the external surface, it is likely that the same species are involved in the grain boundary network, although the mechanisms are likely to be much more complex due to the presence of impurity phases. Further, a different composition of the surface of grains due to cation segregation will lead to a significant modification of the reaction kinetics. The role of impurities is at least twofold; in modifying the defect distribution near the surface and in providing a grain boundary protective coating via the presence of the grain boundary impurity phase. Grain boundary impurity phases and grain surface composition, which vary considerably in different ceramics,[37-40] could therefore be just as critical as grain size or yttria content in determining the stability of sintered Y–TZP.

It is worthwhile considering whether there is any significant difference between moist air and autoclave treatments. It was previously reported by Hughes *et al.*[8,24] that vacancy annealing occurred during moist air treatment of Y–TZP but very little adsorbed water was present during these experiments by contrast to the significant quantities of adsorbed water during the autoclave experiments reported here. During autoclave or moist air treatment both O_2 and water vapour will be present but in different relative ratios. The different relative ratios of the two species in the gas phase as well as the higher pressure in the autoclave environment may well influence the distribution of surface adsorbed species. For example, it would appear that in an autoclave environment significantly more Zr^{3+} is generated suggesting the potential for a much higher density of adsorbed water.[24] If the formation of O_2^-, which is the first step in the reduction of O_2 to O^{2-}, is enhanced in the presence of water on m-ZrO_2[34] then it might be expected that molecular oxygen or superoxide migrates across the surface to a site adjacent to the adsorbed water.[41] Consequently, the rate of reduction of O_2 to O^{2-} will be increased if the density of adsorbed water is higher. On this basis alone, it could be expected that autoclave treatment will result in more rapid transformation to m-phase than moist air treatment.

While the route from O_2 to O^{2-} is conceptually clear, it is unclear what role the decomposition of H_2O has to play. In the case of adsorbed water it might be expected that some surface hydroxyl group are formed, however, surface OH^- was not evident in the XPS suggesting that if OH^- is formed then it must react quickly to give O^{2-} and either H_2 or interstitial H^+. Krouse *et al.*[17] have demonstrated, using ERDA, that hydrogen penetrates the lattice, and given the weight gain and desorption of H_2 from autoclave treated Y–TZP measured by Narita *et al.*[15] it seems likely that interstitial hydrogen is produced. Interstitial hydrogen ions would provide charge balance for the excess O^{2-}.

5 Conclusions

The XRD results indicate that the addition of TiO_2 to Y_2O_3–ZrO_2 as an alloying oxide retards the onset of the t→m transformation during autoclave treatment at 170°C. XPS and SIMS results further indicate that the only oxygen species on the surface of autoclave treated TiO_2–Y_2O_3–ZrO_2 are adsorbed water, superoxide and oxygen anions. XPS results indicate that treatment in an autoclave environment gives rise to the generation of Zr^{3+} sites which co-ordinatively saturate with water. The presence of adsorbed water on the surface increases the rate of formation of O_2^- which, it is assumed, leads to a much larger amount of O^{2-} than would be the case in the absence of the adsorbed water. It is thought that the excess O^{2-} anions anneal anion vacancies thus destabilising the t-phase and promoting the t→m phase transformation. The observed enrichment of Ti^{4+} occurs as a result of the t→m phase transition and does not appear to retard bulk transformation by creating a protective overlayer which retards the t→m phase transformation.

Acknowledgement

The authors would like to thank Dr M. J. Bannister and Prof. G. Petzow for useful discussions, Ms G. Roderick and Mr M. Fergus for assistance with drafting the diagrams and photography. We are also grateful to the University of Queensland for providing time on their surface analysis instrument for SIMS analysis.

References

1. Whalen, P. J., Reidinger, F. & Antrim, R. F., Prevention of low temperature surface transformation by surface recrystallisation in yttria-doped tetragonal zirconia. *J. Am. Ceram. Soc.*, **72** (1989) 319–21.
2. Tsukuma, K., Kubota, Y. & Tsukidate, T., Thermal and mechanical properties of Y_2O_3-stabilised tetragonal zirconia polycrystals. In *Adv. Ceram., Vol. 12. Science and Technology of Zirconia II.* eds N. Claussen, M. Rhule & A. H. Heuer, The American Ceramics Society, Columbus OH., 1984, pp. 382–90.
3. Watanabe, M., Iio, S. & Fukuura, I., Aging behaviour of Y–TZP. *ibid.*, pp. 391–8.
4. Matsui, M., Soma T. & Oda I., Effect of microstructure on the strength of Y–TZP components. *ibid.*, pp. 371–81.
5. Wang, J. & Stevens, R., Surface transformation and

toughening of TZP ceramics by low temperature aging. *Proc. Br. Ceram. Soc.*, **42** (1989) 167–78.
6. Sato T. & Shimada, M., Crystalline phase change in yttria–partially-stabilised zirconia by low temperature annealing. *J. Am. Ceram. Soc.*, **67**(10) (1984) C212–13.
7. Hernandez, M. T., Jurado, J. R., Duran P. & Fierro, J. L. G., Subeutectoid degradation of yttria–stabilised tetragonal zirconia polycrystal and ceria–doped yttria–stabilised tetragonal zirconia polycrystal ceramics. *J. Am. Ceram. Soc.*, **74** (1991) 1254–8.
8. Hughes, A. E., Ciacchi, F. T. & Badwal, S. P. S., Degradation of Y–TZP in moist environments. In *Proceedings of the Fifth International Conference on the Science and Technology of Zirconia*, eds S. P. S. Badwal, M. J. Bannister & R. H. J. Hannink, Technomic Publishing Co., Lancaster, Pennsylvania, 1993, pp. 152–62.
9. Wang J. & Stevens, R., Preferred $ZrO_2(t) \rightarrow ZrO_2(m)$ transformation on the aged surface of TZP ceramics, *J. Mater. Sci. Letts.*, **8** (1989) 1195–8.
10. Lepisto T. T. & Mäntylä, T. A., A model for structural degradation of Y–TZP ceramics in humid atmosphere. *Ceram. Eng. Sci. Proc.*, **10** (1989) 658–67.
11. Lange, F. F., Dunlop G. L. & Davis, B. I., Degradation during aging of transformation-toughened ZrO_2–Y_2O_3 materials at 250°C. *J. Am. Ceram. Soc.*, **69** (1986) 237–40.
12. Sato, T. & Shimada, M., Transformation of yttria-doped tetragonal ZrO_2 polycrystal by annealing in water. *J. Am. Ceram. Soc.*, **68** (1985) 356–9.
13. Yoshimura, M., Noma, T., Kawabata, K. & Sōmiya, S., Role of H_2O on the degradation process of Y–TZP. *J. Mater. Sci.*, **6** (1987) 465–7.
14. Yoshimura, M., Phase stability of zirconia. *Am. Ceram. Soc. Bull.*, **67** (1988) 1950–5.
15. Narita, N., Leng, S. Inada T. & Higashida, K., Environmental effect on phase stability in Y–TZP ceramics. In *Sintering '87*, Proceedings of the 4th International Symposium on Science and Technology of Sintering in Tokyo (1987), eds S. Sōmiya, M. Shimada, M. Yoshimura & R. Watanabe, Elsevier Science Publishers, London, 1988, pp. 1130–5.
16. Kountouros, P. & Petzow, G., Defect chemistry, phase stability and properties of zirconia polycrystals. In *Proceedings of the Fifth International Conference on the Science and Technology of Zirconia*, eds S. P. S. Badwal, M. J. Bannister & R. H. J. Hannink, Technomic Publishing Co., Lancaster, Pennsylvania, 1993, pp. 30–48.
17. Kruse, O., Corstanjen, H. D., Kountouros, P. W., Schubert H. & Petzow, G., Characterization of H_2O–aged TZP by elastic recoil detection analysis (ERDA). In *Proceedings of the Fifth International Conference on the Science and Technology of Zirconia*, eds S. P. S. Badwal, M. J. Bannister & R. H. J. Hannink, Technomic Publishing Co., Lancaster, Pennsylvania, 1993, pp. 163–70.
18. Sato T. & Shimada, M., Control of the tetragonal-to-monoclinic phase transformation of yttria–doped tetragonal ZrO_2 polycrystals (Y–TZP) by annealing in water. *Proc. Br. Ceram. Soc.*, **37** (1986) 151–8.
19. Theunissen, G. S. A. M., Winnubst, A. J. A. & Burggraaf, A. J., Effects of dopants on the sintering behaviour and stability of tetragonal zirconia ceramics. *J. Eur. Ceram. Soc.*, **9** (1992) 251–64.
20. Duran, P., Hernandez, T., Moure, C., Gonzalez, M., Recio, P., Pascual, C. & Jurado, J. R., Aging behaviour properties of SOFC electrolytes. In *Ceramics Today–Tomorrow's Ceramics*, ed. P. Vincenzini, Elsevier Science Publishers, Amsterdam, 1991, pp. 2219–28.
21. Shigematsu, T., Nakao, Y. & Nakanishi, N., Effect of water on the tetragonal to monoclinic phase transition of ZrO_2 with Y_2O_3. In *Shape Memory Materials*, Vol. 9, eds M. Doyama, S. Somiya & R. Chang, Materials Research Society. Pittsburgh, 1989, pp. 549–54.
22. Kountouros, P. & Schubert, H., Bloating Effect During Sintering of TZP. In *Proc. 2nd Europ. Ceram. Soc. Conf.*, Augsburg, 1991.
23. Hughes, A. E. & Badwal, S. P. S., Impurity and yttrium segregation in yttria–tetragonal zirconia. *Solid State Ionics*, **46** (1991) 265–74.
24. Hughes, A. E., Ciacchi, F. B. & Badwal, S. P. S., Role of O^{2-}, OH^- and anion vacancies in the degradation of Y–TZP in moist environments. *J. Mater. Chem.*, **4**(2) (1994) 257–63.
25. Leonov, A. I., Kostikov, Yu. P., Ivanov, I. K., Andreeva, N. S. & Trusova, E. M., The nature of electrical conductivity of solid solutions in the ZrO_2–Y_2O_3 system. *Iz. Akad. Nauk SSSR, Neorg. Mat.*, **16** (1980) 1076–9.
26. Miller, M. L. & Linton, R. W., X-Ray photoelectron spectroscopy of thermally treated SiO_2 surfaces, *Anal. Chem.*, **57** (1985) 2314–19.
27. Dolle, P., Drissi, S., Besançon, M. & Jupille, J., Application of a point-charge model to the O^{2-}, O_2^{2-} and O_2^- ions formed in the presence of Li, K and Cs. *Surf. Sci.*, **269/270** (1992) 687–90.
28. Barr, T. L., An ESCA study of the termination of the passivation of elemental metals. *J. Phys. Chem.*, **82** (1978) 1801–10.
29. De González, C. O. & García, E. A., An X-ray photoelectron spectroscopy study of the surface oxidation of zirconium. *Surf. Sci.*, **193** (1988) 305–20.
30. Morant, C., Sanz, J. M., Galán, L., Soriano, L. & Rueda, F., An XPS study of the interaction of oxygen with zirconium. *Surf. Sci.*, **218** (1989) 331–45.
31. Orera, V. M., Merino, R. I., Chen, Y., Cases, R. & Alonso, P. J., Intrinsic electron and hole defects in stabilized zirconia single crystals. *Phys. Rev. B*, **42** (1990) 9782–9.
32. Azzoni, C. B. & Paleari, A., EPR study of electron traps in X-ray-irradiated yttria–stabilised zirconia, *Phys. Rev. B*, **40** (1989) 6518–22.
33. Morterra, C., Giamello, E., Orio, L. & Volante, M., Formation and reactivity of Z^{3+} centers at the surface of vacuum annealed monoclinic zirconia, *J. Phys. Chem.*, **94** (1990) 3111–16.
34. Giamello, E., Volante, M., Fubini, B., Geobaldo, F. & Morterra, C., *Mater. Chem. Phys.*, **29** (1991) 379.
35. Jackson, P. & Parfitt, G. D., *Trans. Far. Soc.*, **67** (1971) 2469–83.
36. Tanaka, K. & White, J. M., Characterisation of species adsorbed on oxidized and reduced anatase. *J. Phys. Chem.*, **86** (1982) 4708–14.
37. Hughes, A. E. & Badwal, S. P. S., The effects of sintering atmosphere on impurity phase formation and grain boundary resistivity in Y_2O_3–fully stabilized ZrO_2. *J. Eur. Ceram. Soc.*, **10** (1992) 115–22.
38. Hughes, A. E., Segregation in single crystal fully-stabilized yttria–zirconia. *J. Am. Ceram. Soc.*, **78**(2) (1995) 369–78.
39. Ingo, G. M. & Padeletti, G., Segregation aspects at the fracture surfaces of 8 wt% yttria–zirconia thermal barrier coatings, **21** (1994) 450–4.
40. Chaim, R., Brandon, D. G. & Heuer, A. H., A diffusional phase transformation in ZrO_2-4 wt% to Y_2O_3 induced by surface segregation. *Acta Metall.*, **34**(10) (1986) 1933–9.
41. Taylor, R. J. & Humffray, A. A., Electrochemical studies on glassy carbon electrodes: II. oxygen reduction in solutions of high pH (pH > 10). *J. Electroanal. Chem.*, **64** (1975) 63–84.